

Millimeter-Wave and Submillimeter-Wave Imaging for Security and Surveillance

Explosives hidden under clothing can be imaged by submillimeter waves, but millimeter waves are better suited for guiding helicopter navigation in poor weather.

By ROGER APPLEBY, *Member IEEE*, AND RUPERT N. ANDERTON

ABSTRACT | Passive equipments operating in the 30–300 GHz (millimeter wave) band are compared to those in the 300 GHz–3 THz (submillimeter band). Equipments operating in the submillimeter band can measure distance and also spectral information and have been used to address new opportunities in security. Solid state spectral information is available in the submillimeter region making it possible to identify materials, whereas in millimeter region bulk optical properties determine the image contrast. The optical properties in the region from 30 GHz to 3 THz are discussed for some typical inorganic and organic solids. In the millimeter-wave region of the spectrum, obscurants such as poor weather, dust, and smoke can be penetrated and useful imagery generated for surveillance. In the 30 GHz–3 THz region dielectrics such as plastic and cloth are also transparent and the detection of contraband hidden under clothing is possible. A passive millimeter-wave imaging concept based on a folded Schmidt camera has been developed and applied to poor weather navigation and security. The optical design uses a rotating mirror and is folded using polarization techniques. The design is very well corrected over a wide field of view making it ideal for surveillance and security. This produces a relatively compact imager which minimizes the receiver count.

KEYWORDS | Millimeter-wave imaging; security; submillimeter-wave imaging; surveillance; terahertz; 35 GHz; 94 GHz

Manuscript received October 12, 2005; revised March 19, 2007. This work was supported by the U.K. Ministry of Defence. The authors are with QinetiQ Ltd, Malvern WR14 3PS, U.K. (e-mail: rappleby@QinetiQ.com; randerton@QinetiQ.com).

Digital Object Identifier: 10.1109/JPROC.2007.898832

I. INTRODUCTION

In the region of the spectrum below 30 GHz, conventional imaging is impractical due to the large apertures required. It has, however, been known since the 1940s that operating equipment in this part of the spectrum provides excellent penetration of the atmosphere and other obscurants. This has given rise to air defense and surveillance radar systems capable of standoff ranges of hundreds of kilometers. These systems make use of apertures of several meters which are either real or synthetic. Synthetic aperture radar (SAR) uses the motion of the platform on which the radar is mounted to synthesize the aperture. Radars operating at frequencies less than 30 GHz use very mature technology and there are powerful transmitters and well established techniques for data collection and display [1]. In this paper we are primarily concerned with systems which operate at frequencies of greater than 30 GHz and which have smaller apertures.

Above 30 GHz the transmission of the atmosphere varies more strongly as a function of frequency. This variation is primarily caused by the absorption due to water vapor and oxygen and generally increases with frequency. There are relatively transparent windows in the atmosphere which occur at 35, 94, 140, and 220 GHz, and equipments typically operate at these frequencies. The scene being observed will also have optical properties which are frequency dependent and will give rise to contrast in an image. The origin of this contrast is discussed in Section II.

In the millimeter-wave (MMW) region from 30 to 300 GHz (1 cm to 1 mm), imaging systems have been developed. In this waveband both passive and active imaging systems have been demonstrated. They are able to penetrate poor weather for surveillance and also see

through materials such as cloth and polymers for security applications. One example of an active imaging system would be the 94 GHz FMCW radars produced for aircraft landing [2]. The development of passive imaging sensors has lagged behind the development of radar, but over the last ten years the development of low noise receivers using III-V semiconductors such as gallium arsenide and indium phosphide has given rise to systems with good thermal sensitivity. This has made it possible to image in real time with mechanically scanned systems; these are described in Section III-B.

The terahertz region (1–1000 THz) occupies the part of the spectrum between 300 and 0.3 μm and a section of this from 300 GHz–3 THz (1 mm to 100 μm) is the submillimeter-wave (SMMW) region. In this region it has until recently been difficult to develop high-power sources and sensitive detectors. Hu and Nuss [3] reported the first imaging system based on optoelectronic terahertz time-domain spectroscopy. A 100 fs pulse generated from a Ti-sapphire laser incident on semi-insulating gallium arsenide was used to generate terahertz radiation. The radiation after collimation and focusing on to the sample was relayed onto an optically gated dipole detector. This technique is a coherent method enabling images to be generated at different depths in the sample and spectral information to be measured. The atmosphere is strongly absorbing in the SMMW region but short-range applications such as medical imaging, security, and nondestructive evaluation have been reported [4].

A comparison of imaging technology for the MMW and the SMMW regions is constrained to some degree by the difference in their maturity. Ditchfield and England [5] reported the first MMW imaging systems in the United Kingdom, which was 40 years before Hu and Nuss [3] reported a similar demonstration in the terahertz region. The history of MMW technology can be traced back as far as the 1890s, but the first significant activities in this field were conducted in the 1930s [6]. Since then, this technology has continued to develop, with the most rapid advances occurring in recent years.

Prototype passive MMW imaging systems have been developed for poor weather navigation and security scanning. Prototype terahertz systems have also been developed for security screening and are discussed in Section III. Section IV summarizes the comparison of imaging in the SMMW and MMW regions.

II. CONTRAST IN THE SCENE

In an imaging system it is important to understand the origin of the contrast in the scene. In the visible part of the spectrum, where our eyes are most sensitive and the atmosphere is virtually transparent, contrast is derived primarily from the differences in reflectivity between objects and their backgrounds. These objects are surrounded by a hemisphere of sky which illuminates them. Objects have

different reflectivities in different parts of the visible spectrum and so take on different colors. The reflectivity can also be influenced by their surface properties which can be either smooth giving rise to specular reflection, or rough giving rise to diffuse reflection.

The contrast in the scene in any part of the spectrum is a function of the optical properties of the object being imaged and its background. The apparent temperature of an object T_o in the scene is defined by (1). T is the physical temperature of the object, ε its emissivity, T_S is the temperature of the background which is reflected by the object with reflectivity r , T_B is the temperature of the background immediately behind the object, and t is the object's transmission

$$T\varepsilon + T_{Sr} + T_{Bt} = T_o. \quad (1)$$

Imagery can be generated in at least two ways. The first is by receiving natural radiation which has been emitted and reflected from the scene and is known as passive imaging. The second is by transmitting radiation at the scene which after reflection is collected, and is known as active imaging (radar).

Passive MMW images can look similar to visible pictures given an imager with a similar spatial resolution [7], as the reflected component is often large. This is due to two factors: firstly many surfaces are smooth on a wavelength scale and act as specular reflectors and secondly the sky has a low radiation temperature. The sky radiation temperature is typically 100 K on a clear day at the zenith. The cosmic background (5 K) is increased to 100 K by atmospheric emission. When reflectivity approaches zero, as is the case with grass (see Table 2), the apparent temperature will be a function of its physical temperature and will be similar to the ambient temperature.

In active imaging the signature is dominated by reflection, and only the parts of the target which provide a return signal will be detected. A surface which has this property could be normal to the direction of illumination or be a structure such as a corner cube; these are often referred to as scattering centers. Active images are often dominated by speckle and multipath effects but these can be reduced by maximizing the bandwidth and averaging multiple images of the scene. In active and passive imaging, the contrast of an object can have a strong frequency dependence which will result from the atmospheric absorption, its own optical properties, and those of the background.

In the MMW region the spectra of most solids are essentially flat. Gases do, however, have many absorption lines; for example, atmospheric absorption is dominated by the spectra of oxygen and water vapor. This absorption is largely due to rotational modes. These modes are quenched in the liquid phase. Chantray [8] reviews

Table 1 Low-Frequency Absorptions for Typical Ionic, Inorganic Molecular, and Organic Solids

Material	Frequency THz
Ionic Solids	
NaCl	4.29
NaBr	4.2
NaI	3.51
Inorganic Molecular	
HgCl ₂	1.2, 2.25
HgBr ₂	0.93
HgI ₂	0.75
Organic	
C ₆ H _{6(s)} (P=4.1kbar)	2.16, 2.64, 3.0
Polythene	2.37

the SMMW region and discusses solids, liquids, and gases.

The contrast in the scene in the SMMW region is much more like that in the infrared, which is dominated by emission from both target and background. The atmosphere is highly attenuating and the temperature of the sky is increased and is similar to that of the background. This attenuation mitigates against long-range applications but images can be obtained at short range. Most work to date has utilized coherent illumination and detection leading to systems which can measure depth and spectral information. Contrast is therefore derived from the differences in transmission and reflectivity both of which are a function of frequency. Three-dimensional images can also be generated in a similar fashion to radar.

A detailed analysis of the spectra of many different materials and their phases is beyond the scope of this paper. We can, however, observe some general principles and gain some understanding of the impact of spectral properties on target contrast by considering the properties of solids. To illustrate this, the spectra of some typical ionic, inorganic molecular and organic solids are presented in Table 1 [9] and discussed below.

A. Vibrational Spectra

The vibrational spectra of solids are known to fall mostly in the infrared region. Internal molecular vibrations are associated with the infrared fingerprint region of the spectrum and are normally found in the 5 to 100 THz region and will not be discussed here. However of relevance to the MMW and SMMW region are the vibrations that occur below 3 THz and are associated with lattice modes or very low lying internal modes.

Taking sodium halides [10] as typical of ionic solids, we find that they have absorptions from lattice modes as shown in Table 1, all of which are above 3 THz.

There are many classes of organic compounds and here we will consider only two simple compounds, solid

benzene [11] and polythene [12]. Solid benzene is an example of a simple conjugated ring structure. The lowest frequency absorptions which are due to lattice modes are all above 2 THz. Polythene is a relatively simple polymer and, concerning ourselves only with the lattice modes, it can be shown that there are three active modes, one rotary and two translatory, in the far infrared region, the lowest of which appears at 2.3 THz.

Taking the mercuric halides as examples of inorganic molecular solids, we can discuss their low-frequency spectra. Mercuric chloride has two infrared active lattice modes present, one at 2.25 THz and the other at 1.2 THz. Mercuric bromide shows a lattice mode at 0.93 THz and mercuric iodide has its lowest frequency absorption at 0.75 THz.

This overview of the spectral properties of ionic, organic, and inorganic molecular solids only provides an indication of the regions in which spectral absorptions might occur. It can be seen that it is most unlikely that any materials will possess optical activity in the MMW part of the spectrum originating from the vibrational modes of the crystal. This very simple survey indicates that inorganic molecular materials with their relatively heavier atoms will have the lowest absorptions which could be as low as 0.75 THz. The lattice modes in organic materials are likely to be at frequencies greater than 2 THz. SMMW systems can exploit these spectral differences and offer a means of discriminating one material from another. Kemp *et al.* [4] recently reported the spectra of several explosives from 100 GHz to 3 THz and found several features which could be used for identification.

B. Bulk Properties

Objects can also produce contrast in the scene as a function of their bulk optical properties. If they are smooth with respect to the wavelength they will reflect specularly according to Fresnel’s Law [13]. As their surface roughness becomes equal to or greater than the wavelength, they will tend to become more diffuse in nature. The reflectivity of some common materials was measured using a 94 GHz reflectometer [14] and are given in Table 2.

Resonant scattering similar to Mie scattering can also result when there is structure in the object which is similar

Table 2 Normal Incidence Reflectivity at 94 GHz

Material	Reflectivity
Concrete	0.05
Brick	0.1
Slate	0.2
Grass	0.05
Skin	0.4
Metal	~1
Clothing	0.05

Table 3 Atmospheric Attenuation in Clear Air, $T = 20\text{ C}$, $\text{H}_2\text{O} = 7.5\text{ g/m}^3$

Frequency THz	Attenuation db/km
0.035	0.15
0.094	0.6
0.140	2
0.220	8
1	500
10	100

in size to the wavelength. This type of scattering can be confused with spectral absorptions, and great care should be taken interpreting spectral information from materials with such features. At MMW many materials are transparent and their surfaces are smooth when compared to the wavelength. Interference effects resulting from radiation which is reflected from the front and back surface of objects are therefore often observed. At SMMW objects tend to be less transparent. This reduction in transmission can either be a function of absorption due to lattice modes (see Section II-A) or scattering. There surfaces are also more likely to be rough on a wavelength scale, producing diffuse reflectance.

C. Atmospheric Properties

The contrast of an object as observed by an imaging system

$$C(R) = C(0) \left(1 + \frac{b}{r(0)} (\exp(\alpha R) - 1) \right)^{-1} \quad (2)$$

is reduced by the attenuation of the atmosphere according to Koschmeider’s equation [15] where R is range, α is the attenuation coefficient, b is a scattering parameter and r is the apparent averaged reflectivity of target and background. This attenuation has been reported by many different workers [16]. In the region of the spectrum from 10 mm to 20 μm , atmospheric transmission is dominated by absorptions from water and oxygen. There are atmospheric windows with low attenuation and these are centered on the frequencies of 35, 94, 140, and 220 GHz. The attenuation coefficient in the atmosphere is usually quantified in units of dB/km. The attenuation in these windows is shown in Table 3 [17] for clear air and can be compared to the attenuation at 1 and 10 THz. It can be seen that the attenuation at 1 THz is five orders of magnitude greater than at 0.1 THz. This is also shown graphically in Fig. 1.

In poor weather such as rain or fog, this attenuation is further increased as shown in Fig. 2. The plots for drizzle and heavy rain show a knee at a few hundred GHz. Above this frequency the attenuation is one or two orders of magnitude greater than in the MMW region. However, it does remain constant up to 100 THz. The

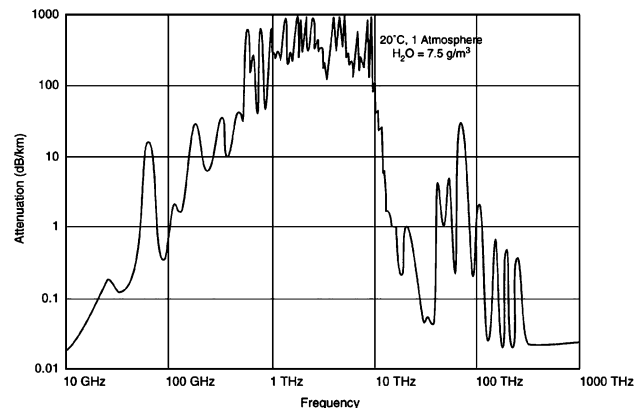


Fig. 1. Atmospheric attenuation clear air.

total attenuation in fog at 10 to 100 THz is approximately 300 dB/km, and this will prevent terahertz systems from being operated at useful ranges in poor weather.

D. Summary

The optical properties of materials in the MMW region have no spectral features, and the contrast in a passive image is generated from the bulk properties of the material. Reflectivity dominates the signature and can produce imagery similar to the visible region when operating outdoors. MMW systems have good performance in fog as the attenuation resulting from the atmosphere can be less than 1 dB/km, and these systems are ideal for imaging through poor weather.

In the region above 1 THz intramolecular vibrations in solids can be seen and can in principle be used to identify materials. The atmosphere also attenuates strongly above 1 THz, and it is unlikely that this region of the spectrum

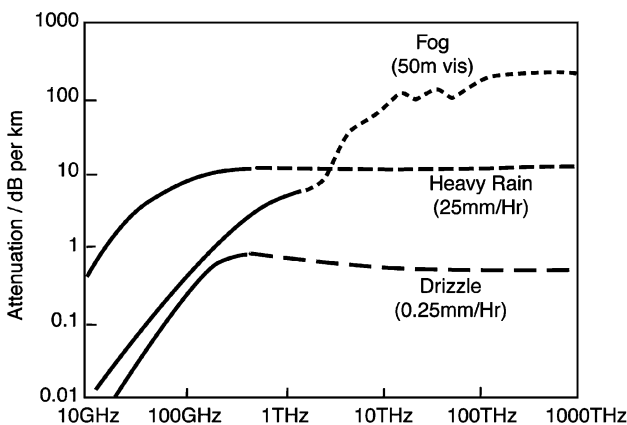


Fig. 2. Atmospheric attenuation in fog and rain.

will be used for surveillance or security applications requiring a large standoff range.

III. IMAGING SYSTEMS

Systems which can image the contrast in a scene have been developed in the MMW and SMMW region. The MMW systems are passive and are based on a real-time mechanical scanning architecture. Terahertz systems have also demonstrated that they can image hidden objects and are an alternative for security applications.

A. Terahertz Imaging

The security applications of terahertz technology were described by Kemp *et al.* [4]. They have developed a terahertz pulse imaging (TPI) imaging technique that works in the frequency range from 0.1 to 10 THz. A TPI system is described which is designed for imaging objects a few centimeters in size. The instrument uses similar principles to those described by Hu and Nuss [3] and is based on a pulsed Ti-sapphire laser. The laser produces 250 fs pulses at 800 nm which are down-converted to terahertz pulses using a biased GaAs wide aperture antenna. The spatial resolution is $\sim 350 \mu\text{m}$ and is diffraction limited. The time resolution is approximately 0.5 ps which corresponds to a depth resolution of 20–40 μm depending on the refractive index of the material.

A portable terahertz imaging system [4] has also been reported. It is approximately 1 m (h) \times 1 m (w) \times 0.5 m (d) and has a flatbed scanner where samples can be placed for analysis. In an alternative configuration the scanned aperture is replaced by an articulated arm which can be used to dynamically interrogate samples.

Kemp reports the 3-D images under multiple layers of clothing of a metal scalpel blade, a square of alumina, an acrylic triangle and a square of SX2 plastic explosive and the images are easily recognizable. Furthermore the absorption spectra for the explosive compounds NT, HMX, PETN, RDX, PE4 and Semtex are reported from 100 GHz to 3 THz. These spectra clearly show that these materials can be discriminated in this spectral range. Paper, cloth, and other similar material were found to be transparent with a flat spectral response. There are therefore good prospects of using terahertz to develop practical systems for detecting hidden explosives but the range is relatively short and the field of regard is small. This technology has also been used to penetrate envelopes to read the type on enclosed documents and could be useful for detecting biological agents.

B. Passive Millimeter-Wave Imaging

The early developments in the United Kingdom which led to real-time systems are described elsewhere [9]. A schematic diagram of a real-time mechanically scanned imaging system [18] is shown in Fig. 3. The optics are

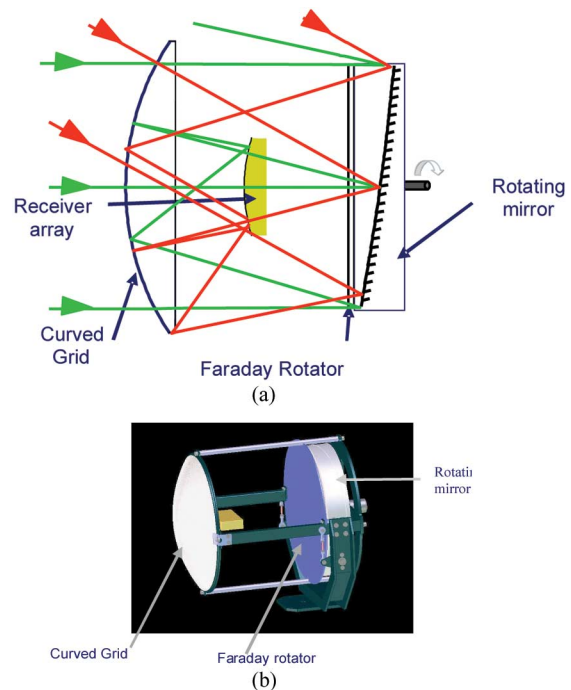


Fig. 3. Real-time mechanically scanned 94 GHz instrument (a) Raytrace (b) CAD representation of imager.

based on a folded Schmidt camera combined with a conical scanner. The folding is done to reduce the size of the system and is achieved using polarization techniques [19]. The main components are an offset rotating mirror, which produces a conical scan pattern, a converging mirror (curved polarizing grid), a free space Faraday rotator which rotates the plane of polarization nonreciprocally by 45° , and an array of receiver modules. The offset rotating mirror and the curved grid are both supported on expanded polystyrene foam. This concept has been used at 94 GHz for poor weather navigation and at 35 GHz for security scanning.

1) *Poor Weather Navigation (94 GHz)*: The operation of helicopters is currently constrained by weather and obscurants such as smoke and dust. At present there is an increasing need to be able to operate 24 h per day and in conditions approaching zero visibility. Passive MMW imaging offers an opportunity to increase the existing operational envelope by providing a means of penetrating obscurants that are opaque in the visible and infrared regions of the spectrum. Operating an imaging sensor effectively from a helicopter, however, can be particularly challenging as this type of platform has a demanding vibration environment.

A prototype 94 GHz imager has been designed to work in this environment [20]. This imager has an aperture of 50 cm, and a raytrace is shown in Fig. 3(a) and a 3-D CAD

in Fig. 3(b). The design is driven by the need to achieve a performance which is as close to the diffraction limit as possible. However, obscuration, aberrations, and build tolerances will result in a performance somewhat less than the ideal. These contributions must be taken into account when setting the tolerances on the design [21]. In the central two-thirds of the field of view, the optical path length is corrected to better than a quarter of a wavelength. Over this field of view the imager has diffraction limited performance, which is essential to ensure that good spatial resolution is maintained.

The mechanical accuracy of an optical system will always affect its performance. In optical design this is referred to as tolerancing. Tolerances are additive but they are statistically independent and so they add as the square root of the sum of the variances [22], [23] as shown in (3)

$$b = \sqrt{\sum_{i=1}^n x_i^2}. \quad (3)$$

Here the tolerance budget for the i th component is x_i and the total tolerance budget is b . Tolerancing an optical design aims to minimize the impact that small deviations from the ideal shape, position, and surface finish will have on the final performance of the system. Obviously as the total budget is increased the optical performance of the system will degrade.

Static geometric or build tolerances fall into four types: linear position, surface, decenter, and tilt. As well as the build tolerances (static geometric tolerances), we must also consider dynamic tolerances. Dynamic tolerances are the tolerances due to relative motion of the optical components in a vibration environment. These tolerances have been calculated and were reported [21]. The demanding tolerances are the surface finish and the form of the grid and rotating mirror. The form of the component is a direct result of the machining method used. All of the expanded polystyrene foam components are manufactured on conventional milling machines. For conventional materials an accuracy of 0.025 mm is easily achievable; however, when machining foams such as expanded polystyrene, plastic deformation can occur. This is minimized by using high density foam (30 g/lit) and optimizing the machining conditions. Accuracies have routinely been achieved of better than 0.1 mm radius, which is compatible with the required build tolerance.

The quality of the surface finishes in this design is to some extent determined by the surface finish obtained on the machined expanded polystyrene foam. It is, however, improved by coating with thin film materials, which effectively smooth out undulations in the polystyrene. This

imager when operated under simulated helicopter vibration was shown to image within specification and has demonstrated that it is possible for these systems to function under harsh vibration environments if they are designed correctly.

To cover the $52^\circ \times 26^\circ$ field of view, approximately 150 receivers are required. Monolithic microwave integrated circuits (MMICs) are a key enabling technology for realizing the receiver modules since this approach allows excellent repeatability between receivers, reduces cost and allows a compact form-factor to be achieved. A custom chip set has been developed and is described by Barnes *et al.* [24].

2) *Security (35 GHz)*: Both passive and active systems have been reported at 35 GHz. An active imager based on a 3-D holographic radar technique has been demonstrated by Sheen, McMakin, and Hall [25] and produces good quality images. Sinclair *et al.* [26] reported a passive imager with a 1.6 m aperture that is based on the folded conical scan imager described above. This imager has a field of view of $20^\circ \times 10^\circ$ degrees, which will cover an adult at 4 m.

It is similar to the W band variant but uses a meanderline quarter-wave plate to rotate the plane of polarization. A custom receiver module based on MMIC technology has also been developed for this application and is described by Barnes *et al.* [24].

This imager has been used to collect imagery of people both indoors and outdoors as shown in Fig. 4. Metal objects which have a high reflectivity (see Table 2) can be seen with good contrast against the body which only has a reflectivity of about 40%. In Fig. 4(a) a metal gun with high contrast can be seen on the right thigh of the person on the right of the image. Outdoors these differences in reflectivity are observed as a result of the cold sky, which subtends a large solid angle and is reflected by the object.

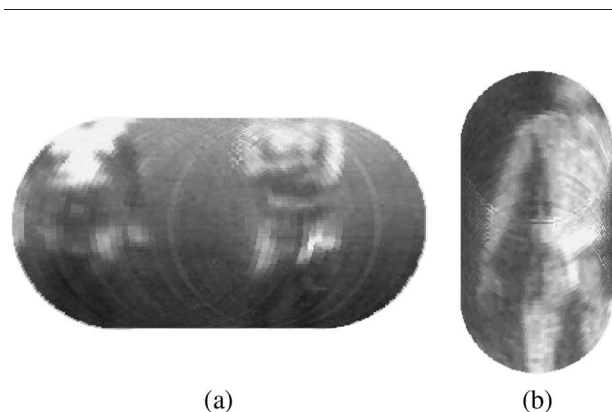


Fig. 4. 35 GHz imagery. (a) Outdoor. (b) Indoor.

Indoor imaging cannot use the cold sky as a source of image contrast as building materials are opaque in the MMW region. It is therefore necessary to use artificial illumination to mimic the sky. A method for achieving this was reported by Coward [27] who used MMW diffuse panels which emitted a low level of incoherent radiation to illuminate a person over a large solid angle. Images from this system are shown in Fig. 4(b) where a metal gun can clearly be seen.

IV. SUMMARY

Atmospheric transmission will severely limit the ability of SMMW systems to perform at any reasonable stand-off range. Poor weather navigation will therefore be dominated by systems operating at MMW or lower frequencies.

Clothing is highly transparent in both the SMMW and MMW regions, and so threat objects hidden under clothing can be imaged, but there is no spectral information available to identify materials in the MMW waveband. Imaging in the SMMW region provides a

means of discriminating between different types of material, and there are good prospects of using SMMW to develop practical systems for detecting and identifying hidden explosives. Furthermore, terahertz sensors which use a coherent pulsed source and time gated detector can measure depth and hence produce 3-D imagery. This is not possible with passive MMW imagers; however, 3-D imaging has been demonstrated with active MMW systems.

Real-time MMW imaging systems have been enabled by MMIC technology and novel optical designs. MMIC technology is available at 35 and 94 GHz and can provide large numbers of receivers at relatively low cost, but such devices are not currently available at THz frequencies. Novel optical designs based on Schmidt telescopes with conical scanners have been used with MMIC receiver technology to demonstrate imaging systems with wide fields of view which can image in real time. These imagers have been used to demonstrate navigation in poor weather and to collect indoor and outdoor imagery of weapons and contraband hidden under clothing. ■

REFERENCES

- [1] M. I. Skolnik, *Radar Handbook*. New York: McGraw Hill, 1970.
- [2] *Autonomous Landing Guidance*. [Online]. Available: http://www.eis.na.baesystems.com/brochures/pdfs/autonomous_landing_guidance.pdf
- [3] B. B. Hu and M. C. Nuss, "Imaging with terahertz," *Opt. Lett.*, vol. 20, no. 16, pp. 1716–1718, 1995.
- [4] M. C. Kemp, P. F. Taday, B. E. Cole, J. A. Cluff, A. J. Fitzgerald, and W. R. Tribe, "Security applications of terahertz technology," *Proc. SPIE*, vol. 5070, pp. 44–52, 2003.
- [5] C. R. Ditchfield and T. S. England, "Passive detection at Q band," in *RRE Memo.*, p. 1124, 1955.
- [6] J. C. Wiltse, "History of millimeter and submillimeter waves," *IEEE Trans. Microw. Theory Tech.*, vol. MTT-32, no. 9, pp. 1118–1127, Sep. 1984.
- [7] R. Appleby, D. G. Gleed, R. N. Anderton, and A. H. Lettington, "Advances in passive millimeter wave imaging," *Proc. SPIE*, vol. 2211, pp. 312–317, 1994.
- [8] G. W. Chantry, *Submillimeter Spectroscopy*. New York: Academic, 1971.
- [9] R. Appleby, "Passive millimeter wave imaging and how it differs from terahertz imaging," *Phil. Trans. R. Soc. Lond. A*, vol. 362, pp. 379–394, 2004.
- [10] S. S. Mitra and P. J. Giellisse, "Infrared spectra of crystals," *AFCRL-69-395*, 1965.
- [11] D. M. Adams and R. Appleby, "Vibrational spectroscopy at very high pressures, part 18. Three solid phases of benzene," *J. Chem. Soc. Faraday Trans. II*, vol. 73, no. 12, pp. 1896–1905, 1977.
- [12] S. Krimm and M. I. Bank, "Assignment of the 71 cm^{-1} band in polyethylene," *J. Chem. Phys.*, vol. 42, pp. 4059–4060, 1965.
- [13] P. Lorrain and D. Corson, *Electromagnetic Fields and Waves* 2nd ed. San Francisco, CA: Freeman, 1970.
- [14] R. Appleby and M. Leeks-Musselwhite, "Millimetre-wave reflectometer," *Proc. SPIE*, vol. 4719, pp. 402–408, 2002.
- [15] Y. LeGrand, *Light Colour and Vision*. London, U.K.: Chapman & Hall, 1968.
- [16] "Attenuation by atmospheric gases," ITU-R P.676-5, 2001.
- [17] C. H. Zufferey, "A study of rain effects on electromagnetic waves in the 1–600 GHz ranges," Master's Thesis, Univ. Colorado, Boulder, 1972.
- [18] A. H. Lettington, P. Papakosta, and D. Dunn, "Opto-mechanical scanners for passive millimeter-wave imaging," *Proc. SPIE*, vol. 4032, pp. 74–79, 2000.
- [19] R. Appleby, R. N. Anderton, N. A. Salmon, G. N. Sinclair, J. R. Borrill, P. R. Coward, P. Papakosta, A. H. Lettington, and D. A. Robertson, "Compact real-time (video rate) passive millimeter-wave imager," *Proc. SPIE*, vol. 3703, pp. 13–19, 1999.
- [20] R. Appleby, "Mechanically scanned real time passive millimeter wave imaging at 94 GHz," *Proc. SPIE*, vol. 5077, pp. 1–6, 2003.
- [21] R. Appleby, R. N. Anderton, N. Thomson, and J. W. Jack, "The design of a real time 94 GHz passive millimeter wave imager for helicopter operations," *Proc. SPIE*, vol. 5619, pp. 38–46, 2004.
- [22] W. J. Smith, *Modern Lens Design—A Resource Manual*. New York: McGraw-Hill, 1992, ch. 23, pp. 431–440.
- [23] *OSLO Version 5 Optical Reference for OSLO Six/OSLO Pro*. Sinclair Optics Inc., Pittsfield, NY, 1996.
- [24] A. R. Barnes, P. Munday, R. Jennings, M. Moore, M. Black, R. Appleby, R. N. Anderton, G. N. Sinclair, and P. R. Coward, "MMIC technology and its application in passive mm-wave imaging systems," in *Proc. 3rd ESA Workshop Millimetre Wave Technology and Applications*, 2003, pp. 543–547.
- [25] D. M. Sheen, L. McMakin, and T. E. Hall, "Three-dimensional millimeter-wave imaging for concealed weapon detection," *IEEE Trans. Microwave*, vol. 49, no. 9, pp. 1581–1592, Sep. 2001.
- [26] G. N. Sinclair, R. Appleby, P. R. Coward, and S. Price, "Millimeter-wave imaging for security scanning," *Proc. SPIE*, vol. 4032, pp. 40–45, 2000.
- [27] P. R. Coward and R. Appleby, "Development of an illumination chamber for indoor millimeter-wave imaging," *Proc. SPIE*, vol. 5077, pp. 54–61, 2003.

ABOUT THE AUTHORS

Roger Appleby (Member, IEEE) received the B.Sc. degree in chemistry from Leicester University, U.K., in 1974 and the Ph.D. degree (dissertation title: “Vibrational spectroscopy under pressure”) in 1977. He completed a postdoctoral study on laser light scattering from solutions and liquid crystals at the University of Queensland, Australia, from 1977 to 1979.



He joined the UK MoD and carried out research into image intensifiers, thermal imagers and lasers. He currently leads the passive millimeter-wave imaging team at QinetiQ, Malvern, U.K. His team has pioneered the use of real-time mechanically scanned passive millimeter-wave imagers for security and poor weather surveillance. At 35 GHz this technology has been used to scan PVC sided trucks at channel ports in Europe for the detection of illegal immigrants and was also used to construct a portal for imaging people in the indoor environment. At 94 GHz it has been applied to standoff to security scanning and helicopter collision avoidance. He chaired a NATO panel TG14 on Passive and active millimeter-wave imaging.

Dr. Appleby is a QinetiQ Senior Fellow.

Rupert N. Anderton received the B.A. degree in physics from Oxford University, U.K., in 1989 and the Ph.D. degree (dissertation title: “Design and Manufacturing Concepts for a Real Time Passive Millimeter-Wave Imager”) from Reading University, U.K., in 1999.



He joined RSRE (then part of the U.K. Ministry of Defence) in 1989 and has been carrying out research into passive millimeter-wave sensing since then. Working as part of Dr. Appleby’s team at QinetiQ (successor organization to RSRE), Malvern, U.K., he currently leads the research into optics for passive millimeter-wave imagers. He was responsible for the optics for the 35 GHz systems used to scan soft-sided lorries at the channel ports, the 35 GHz people screening portal, the 94 GHz helicopter collision avoidance imager and the 94 GHz standoff security scanner. Dr Anderton also leads the research into nonimaging passive millimeter-wave sensors for standoff detection of person-borne explosive devices.

Dr. Anderton is a QinetiQ Fellow.